Research Article

Cancer Prevention Research

Topically Applied Carvedilol Attenuates Solar Ultraviolet Radiation Induced Skin Carcinogenesis

Kevin M. Huang[1], Sherry Liang[1], Steven Yeung[1], Etuajie Oiyemhonlan[1], Kristan H. Cleveland[1], Cyrus Parsa[2,3], Robert Orlando[2,3], Frank L. Meyskens Jr[4], Bradley T. Andresen[1], and Ying Huang[1]

Abstract

In previous studies, the β-blocker carvedilol inhibited EGF-induced epidermal cell transformation and chemical carcinogen-induced mouse skin hyperplasia. As exposure to ultraviolet (UV) radiation leads to skin cancer, the present study examined whether carvedilol can prevent UV-induced carcinogenesis. Carvedilol absorbs UV like a sunscreen; thus, to separate pharmacological from sunscreen effects, 4-hydroxycarbazole (4-OHC), which absorbs UV to the same degree as carvedilol, served as control. JB6 P^+ cells, an established epidermal model for studying tumor promotion, were used for evaluating the effect of carvedilol on UV-induced neoplastic transformation. Both carvedilol and 4-OHC (1 μmol/L) blocked transformation induced by chronic UV (15 mJ/cm^2) exposure for 8 weeks. However, EGF-mediated transformation was inhibited by only carvedilol but not by 4-OHC. Carvedilol (1 and 5 μmol/L), but not 4-OHC, attenuated UV-induced AP-1 and NF-κB luciferase reporter activity, suggesting a potential anti-inflammatory activity. In a single-dose UV (200 mJ/cm^2)-induced skin inflammation mouse model, carvedilol (10 μmol/L), applied topically after UV exposure, reduced skin hyperplasia and the levels of cyclobutane pyrimidine dimers, IL1β, IL6, and COX-2 in skin. In SKH-1 mice exposed to gradually increasing levels of UV (50–150 mJ/cm^2) three times a week for 25 weeks, topical administration of carvedilol (10 μmol/L) after UV exposure increased tumor latency compared with control (week 18 vs. 15), decreased incidence and multiplicity of squamous cell carcinomas, while 4-OHC had no effect. These data suggest that carvedilol has a novel chemopreventive activity and topical carvedilol following UV exposure may be repurposed for preventing skin inflammation and cancer. *Cancer Prev Res; 10(10); 598–606. ©2017 AACR.*

Introduction

β-Adrenergic receptor (β-AR) antagonists, commonly called β-blockers, are usually used for cardiovascular disorders and act via inhibiting catecholamines, i.e., epinephrine and norepinephrine, from triggering the body's "fight or flight" response to stress (1). Recent evidence suggests that catecholamines, by activating β-ARs, also play a role in carcinogenesis including skin carcinogenesis, possibly through inducing DNA damage (2), promoting transformation (3, 4), and inhibiting cutaneous immunity (5). β-ARs are expressed in various cell types of human skin. Keratinocytes, the cells that make up the majority of the epidermis, express only the β2-AR while melanocytes express both β1- and β2-ARs (6, 7). Benign melanocytic nevi, atypical nevi, and malignant melanomas express β1- and β2-ARs, and expression of these receptors is greatest in malignant tumors (8). Ultraviolet (UV) irradiation can increase the secretion of epinephrine from keratinocytes while melanocytes synthesize norepinephrine but are unable to produce epinephrine (9). In melanocytes, the signaling through β-ARs promotes pigmentation in response to epinephrine secreted from the neighboring keratinocytes (6). Thus, catecholamines and UV radiation may synergistically act on the skin microenvironment to promote carcinogenesis.

Recent clinical and preclinical investigations have provided evidence that the use of β-blockers in combination with chemotherapy or radiotherapy reduced metastasis and prolonged the survival of patients with multiple cancers (10–19). For melanoma, epidemiological studies indicate that long-term use of β-blockers reduced progression and mortality (20, 21). However, the association between the use of β-blockers with cancer incidence is infrequently investigated, and their effects on cancer prevention remain controversial (22–24). Also, most of these studies focused on developed tumors, which are not the ideal model to evaluate the preventive effects of β-blockers. Interestingly, long-term use of the β-blocker carvedilol is associated with reduced risk of many cancer types in a recent population-based cohort study (25), which is the largest retrospective cancer incidence study focusing on a single β-blocker involving 6,771 carvedilol users and the same number of non-user controls.

Carvedilol is a third-generation receptor subtype nonselective β-blocker with antioxidant and anti-inflammatory properties (26–28). Previous preclinical studies established carvedilol-mediated chemopreventive effects via inhibition of EGF-induced

[1]Department of Pharmaceutical Sciences, College of Pharmacy, Western University of Health Sciences, Pomona, California. [2]College of Osteopathic Medicine of the Pacific, Western University of Health Sciences, Pomona, California. [3]Department of Pathology, Beverly Hospital, Montebello, California. [4]Departments of Medicine, Biological Chemistry, Public Health and Epidemiology, Chao Family Comprehensive Cancer Center, University of California, Irvine, California.

Note: Supplementary data for this article are available at Cancer Prevention Research Online (http://cancerprevres.aacrjournals.org/).

Corresponding Author: Ying Huang, Western University of Health Sciences, 309 East 2nd Street, Pomona, CA 91766. Phone: 909-469-5220; Fax: 909-469-5600; E-mail: yhuang@westernu.edu

doi: 10.1158/1940-6207.CAPR-17-0132

AACR

transformation of the non-tumorous mouse epidermal cell line JB6 Cl 41-5a (JB6 P^+) and reduction of 7,12-dimethylbenz(α) anthracene (DMBA)-induced epidermal hyperplasia in mice (29). Although the aforementioned studies are models of skin carcinogenesis, the effect of carvedilol should be examined in a more clinically relevant model—skin carcinogenesis induced by UV. Thus, in the present study, we tested the hypothesis that carvedilol prevents UV-induced skin cancer.

Materials and Methods

Compounds

Carvedilol was purchased from Tocris Bioscience. 4-Hydroxycarbazole (4-OHC) and 1,2-dimethoxybenzene was purchased from Sigma-Aldrich and epidermal growth factor (EGF) from Peprotech. Carvedilol and 4-OHC were reconstituted in dimethyl sulfoxide (DMSO) used *in vitro* or in acetone used *in vivo*, whereas EGF was prepared in PBS. All stocks are stored in −20°C and diluted right before each use.

Cell culture

JB6 Cl 41-5a (JB6 P^+), purchased from ATCC in 2011, were cultured as described in the manufacturer's instruction with modification of using media containing 4% heat-inactivated fetal bovine serum. HEK-293 cells were also obtained from ATCC in 2007 and cultured in Dulbecco's MEM (Genesee Scientific) supplemented with 10% fetal bovine serum (Genesee Scientific) and 1% penicillin/streptomycin (Invitrogen). Authentication has not been done by the authors. The described experiments were conducted using cells of less than 10 passages after thawing. All cells from cell culture-related experiments were incubated in a humidified atmosphere of 37°C and 5% CO_2/95% air.

UV–Vis spectral analysis

Compounds were reconstituted in DMSO to a final concentration of 1 mmol/L ($n = 4$) and subjected to complete UV–Vis spectral analysis using NanoDrop 2000c (Thermo Scientific). DMSO served as a blank with 750 nm set to zero and subsequently used as a vehicle control.

UV light source

The UV lamps emitting UVB (280–320 nm; 54% of total energy), UVA (320–400 nm; 37% of total energy), UVC (100–280 nm; 2.0% of total energy) and Visible light (400–450 nm; 7.0% of total energy; catalog numbers #95-0042-08 and #95-0043-13; UVP; Supplementary Fig. S1) were used to irradiate *in vitro* and *in vivo* experiments. Stable power output (mW/cm^2) was measured using a UVX radiometer (#97-0015-02, UVP) coupled with a sensor with a calibration point of 310 nm (UVX-31, #97-0016-04, UVP), and exposure time was calculated using the following formula: dose (mJ/cm^2) = exposure time (s) × output intensity (mW/cm^2). Quality control of the lamps and exposure time were calculated and monitored before each use of the lamps to account for changes in power output over time.

Anchorage-independent growth assay of JB6 P^+ cells promoted by EGF or UV

EGF-mediated transformation of JB6 P^+ cells was conducted in 96-well plates as previously described (29). Low-dose UV irradiation was used to transform the JB6 P^+ cells following a modified method (30). In brief, radiant doses of 15 mJ/cm^2 UV was applied to the cells in PBS three times per week for a total of 8 weeks. The vehicle control, 1 μmol/L carvedilol, or 1 μmol/L 4-OHC were added to the culture media which was replenished after each irradiation. The cells were split upon reaching 80% confluence. After 8 weeks, cell transformation was confirmed by the soft agar assay, without the addition of any promoters or drugs.

Luciferase reporter gene assay

HEK-293 cells were transfected with pRL-TK-Luc *Renilla* luciferase (Promega) and pGL4.22-AP1 (gift, Dr. David Sanchez; Western University of Health Sciences, Pomona, California) or pGL4.22-NF-κB (Promega) plasmids at a ratio of 1:30 using FuGENE HD Transfection Reagent (Roche Applied Science). Twenty-four hours later, the cells were exposed to 25 mJ/cm^2 UV and incubated in fresh growth medium containing test compounds for an additional 5 or 24 hours for NF-κB and AP-1, respectively. Cell lysates were analyzed by the dual luciferase reporter gene assay (Promega) with *Renilla* luciferase serving as a normalization factor.

Acute UV exposure *in vivo* study

All animal studies were carried out under the recommendations and guidelines established by Western University of Health Sciences' Institutional Animal Care and Use Committees which approved these studies. Mice had access to water and food *ad libitum* and housed on a 12-hour light/dark cycle with 35% humidity. SKH-1 hairless mice were randomly divided into 5 groups; $n = 4$ per group for non–UV-exposed controls and $n = 6$ for mice exposed to 200 mJ/cm^2 UV. The groups are: (i) vehicle-treated control, (ii) 10 μmol/L carvedilol-treated control, (iii) UV-exposed followed by vehicle treatment, (iv) 2-hour pretreatment with 10 μmol/L carvedilol then UV-exposed, and (v) UV-exposed followed by 10 μmol/L carvedilol treatment. The volume for topical treatment was 200 μL with acetone as the solvent. The mice were euthanized at 6 or 24 hours after UV exposure, and dorsal skin samples were measured then excised and snap frozen.

Cyclobutane pyrimidine dimer (CPD) dot blot analysis

Genomic DNA was isolated from dorsal skin samples by using QIAamp DNA Mini Kit (Qiagen). The DNA samples (100 ng) were vacuum-transferred to a nitrocellulose membrane (0.45 μm, Thermo Scientific) using a Bio-Dot SF microfiltration apparatus (Bio-Rad). CPDs were detected by immunoslot blot using anti-CPD monoclonal antibody (Kamiya). After the immunoslot blot assay, total DNA amounts loaded onto the membrane were visualized by SYBR-Gold (Invitrogen) staining, and these values were used to normalize the CPD values.

Western blot analysis

Protein was extracted from skin tissue by grinding liquid nitrogen frozen skin into a fine powder with a pre-chilled mortar and pestle before addition of RIPA lysis buffer (Santa Cruz) containing PMSF, Na_3VO_4, and protease inhibitors. The tissues were further homogenized using an OMNI Tissue Master 123 handheld homogenizer. Protein (30 μg) were resolved by 10% SDS-PAGE and transferred to a nitrocellulose membrane. 1:1,000 anti-COX-2 (Cayman Chemicals) and anti–β-actin (Cell Signaling) antibodies in 5% non-fat milk and 5% sodium azide were applied to the membrane overnight, washed six times, and then

exposed to goat anti-rabbit IgG-HRP (Cell Signaling Technologies) diluted 1:20,000 in 5% non-fat milk at room temperature for 60 minutes. Membranes were visualized with SuperSignal West Pico Chemiluminescent Substrate (Thermo Fisher).

Quantitative RT-PCR analysis

Total RNA was isolated from whole skin tissue using TRIzol (Thermo Fisher) and RNeasy Mini kit (Qiagen). cDNA was obtained with the High Capacity cDNA Reverse Transcriptase Kit (Thermo Fisher). cDNA and PerfeCTa SYBR Green Supermix (Quanta Biosciences, Inc.) were combined with primers for mouse Il6, Il1b, and β-actin (The primer sequences are available upon request). Real-time PCR was performed on a CFX96 Real-time thermal cycler detection system (Bio-Rad), and analyzed with the $2^{-\Delta\Delta ct}$ with β-actin as the normalization control.

UV-induced murine skin tumorigenesis

A total of 42 six-week-old female SKH-1 mice (Charles River) were randomly divided into six groups. The groups were (i) $n = 4$ non-UV exposure vehicle treated, (ii) $n = 4$ non-UV exposure carvedilol treated, (iii) $n = 4$ non-UV exposure 4-OHC treated, (iv) $n = 10$ UV-exposed vehicle treated, (v) $n = 10$ UV-exposed carvedilol treated, and (vi) $n = 10$ UV-exposed 4-OHC treated. Mice were topically treated with 200 μL acetone (vehicle), 10 μmol/L carvedilol or 4-OHC dissolved in 200 μL acetone three times per week for 2 weeks before UV exposure. The mice were irradiated with gradually increasing levels of UV 3 times a week for 25 weeks with an initial dose of 50 mJ/cm^2 that was increased each week by 25 mJ/cm^2 to 150 mJ/cm^2, which continued for the duration of the experiment. The treatment regimen was applied after UV irradiation and continued throughout the experiment. During the UV exposure mice roamed freely in acrylic cages on a rotating platform with rotational placement ensuring consistent and equal dorsal distribution of UV irradiation. Tumors of at least 1 mm in diameter were counted and measured weekly. At the end of the study, the mice were euthanized, and tumorous and non-tumorous skin samples were excised and fixed in 10% formalin for pathological analysis. Hematoxylin and eosin (H&E)-stained sections of the tumors were examined by a board-certified pathologist.

Statistical analysis

Data are expressed as a mean ± standard deviation unless stated otherwise. All plots were made using GraphPad Prism, and statistical analysis was conducted in GraphPad Prism and NCSS 2007. Specific statistical tests are detailed in the figure legends or text; for data dealing with tumor number, data are reported as median ± median absolute deviation (MAD), and nonparametric analysis was used for statistical quantification.

Results

4-OHC as a sunscreen control for carvedilol

The UV absorption spectrum of carvedilol and its non-β-ethanolamine R-groups 4-OHC and 1,2-dimethoxybenzene was examined to identify a compound that may serve as a UV absorption control in the proceeding studies. As can been seen from Fig. 1A, the UV absorption profile of carvedilol is completely mimicked by equimolar concentrations of 4-OHC. Because 4-OHC lacks the required β-ethanolamine component of β-blockers, it can serve as a UV absorption (sunscreen) control. The absorption profile covers most of the emitted spectrum of the UV lamps used throughout this study (Supplementary Fig. S1). However, it is unclear whether interacting with β-AR is the mechanism for the chemopreventive properties of carvedilol. Therefore, the concentration-response effects of carvedilol and 4-OHC on EGF-mediated transformation of JB6 P$^+$ cells were examined (Fig. 1B). As previously described, carvedilol inhibited EGF-induced JB6 P$^+$ cell transformation in a dose-dependent manner (29), but 4-OHC had no effect. Thus, 4-OHC can serve as a sunscreen control in following experiments involving UV, allowing for separating the pharmacological and UV absorption properties of carvedilol.

Effects of carvedilol or 4-OHC on UV-induced JB6 P$^+$ cell transformation

As 4-OHC absorbs UV irradiation, it is expected that 4-OHC will have some degree of UV protection, while carvedilol is hypothesized to provide greater preventive activity against UV-induced effects due to its pharmacological activity. This hypothesis was first tested in the JB6 P$^+$ cell transformation assay using UV as the tumor promoter because low and re-occurring dosages

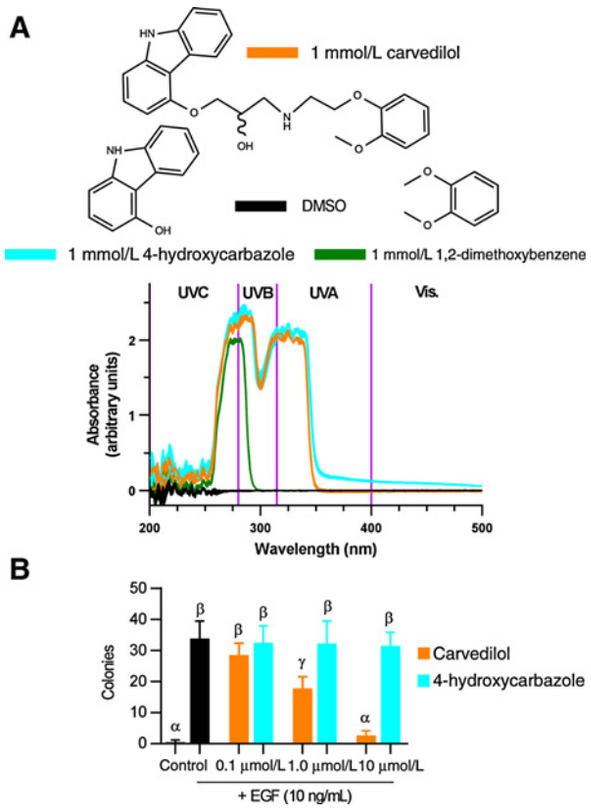

Figure 1.

Establishing a sunscreen control for carvedilol. **A,** Structures of carvedilol and its potential UV absorption moieties are provided along with the key for the UV absorption spectrum shown near the structures. The thickness of the lines represents the mean ± SD; $n = 4$. **B,** Effect of carvedilol and 4-OHC on EGF-induced neoplastic transformation of JB6 P$^+$ cells. Data are expressed as mean ± SD; $n = 8$. Bars with different Greek letters are statistically different ($P < 0.001$) as per one-way ANOVA with Tukey–Kramer *post hoc* test.

of UV irradiation can lead to malignant transformation of JB6 P^+ cells (30). Treating JB6 P^+ cells with 15 mJ/cm^2 UV three times a week for 8 weeks then plating the cells in agar with growth media without any promoter or drugs resulted in more colonies than EGF as the promoter (48 ± 4 vs. 35 ± 4, $P = 0.002922$, respectively; data expressed as median ± median absolute deviation (MAD)). Incubation with 1 μmol/L carvedilol or 1 μmol/L 4-OHC for the duration of experimental paradigm, except during UV exposure, statistically reduced chronic UV-induced colony formation by 64% and 59%, respectively (Fig. 2). Although carvedilol appears more effective than 4-OHC, it is not statistically different.

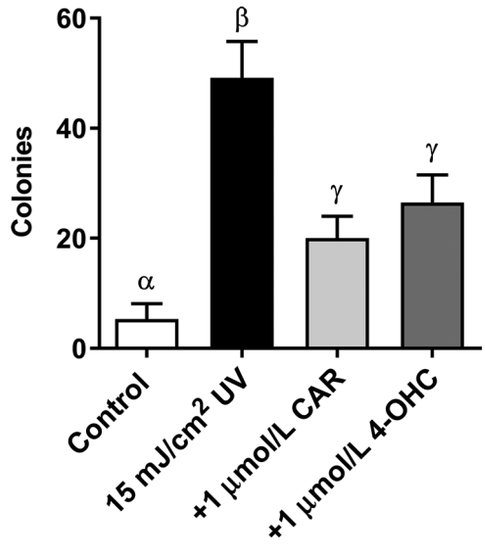

Figure 2.
Effect of carvedilol and 4-OHC on UV-induced JB6 P^+ cell transformation. JB6 P^+ cells were exposed to 15 mJ/cm^2 UV 3 times per week for a total of 8 weeks in the presence or absence of test compounds then plated in the soft agar without any additional ligands; control cells were passaged along with the UV-treated cells. Data are expressed as mean ± SD; $n = 6$. Bars with different Greek letters are statistically different ($P < 0.05$ as well as $P < 0.001$) as per one-way ANOVA with Tukey–Kramer *post hoc* test.

Effects of carvedilol or 4-OHC on UV-induced NF-κB and AP-1 activation

The transcription factor activator protein-1 (AP-1) and NF-κB are principal mediators of skin carcinogenesis activated by UV irradiation (31, 32). To begin exploring the molecular mechanisms underlying the observed effects of carvedilol, UV-mediated activation of AP-1 and NF-κB were evaluated by dual luciferase assays in HEK-293 cells. As shown in Fig. 3, a single low dose of UV (25 mJ/cm^2) was sufficient to activate the transcription of NF-κB and AP-1. Carvedilol, but not 4-OHC, inhibited UV-mediated transcriptional activity of NF-κB and AP-1 when administered after UV exposure. To further confirm that carvedilol, but not 4-OHC, acts through a pharmacological mechanism, TNFα- and EGF-mediated NF-κB and AP-1 activation, respectively, were examined by dual luciferase assays in the absence and presence of carvedilol and 4-OHC. The results (data not shown) are similar to Fig. 3, where carvedilol, but not 4-OHC, inhibits NF-κB and AP-1 activation. These data further demonstrate that the observed UV-protective effects are pharmacological in nature and are not completely due to a sunscreen effect.

Effects of topically applied carvedilol in a short-term UV mouse model

The effects of carvedilol on UV-induced NF-κB activation supports its anti-inflammatory activity. Although antioxidant and anti-inflammatory effect of carvedilol has been reported related to hypertension (28), its contribution to UV induced inflammation, a known factor leading to skin carcinogenesis (33, 34), is unclear. A short-term UV exposure model was chosen to address this question *in vivo*. A single dose of 200 mJ/cm^2 UV was utilized to examine proximal effects of carvedilol treatment in SKH-1 mice after 6 and 24 hours. To investigate treatment protocols, the mice were treated with topical carvedilol (10 μmol/L) 2 hours before or immediately after UV irradiation. These two groups mirror a prophylactic treatment, such as the use of sunscreen, and treatment for a sunburn, respectively. Bifold thickness of dorsal epidermal skin was measured before and after UV treatment to examine the effect of carvedilol on UV-induced skin edema/hyperplasia. As expected, UV induced a rapid change in skin thickness (45% and 56% increase, 6 hours or 24 hours after irradiation, respectively; Supplementary Fig. S2), and the control groups not exposed to UV showed no change. Only carvedilol treatment immediately after UV exposure ("postCAR"), when examined after 24 hours, showed a statistical decrease in bifold skin thickness.

UV exposure induces DNA damage in skin epidermis predominantly through the formation of CPD. The level of CPD was detected 6 hours after UV exposure and was visibly reduced after 24 hours (Fig. 4A). Treatment by carvedilol before or after UVB exposure resulted in 50.8% and 62.9% reduction in CPD, respectively, within 6 hours ($P < 0.001$ compared with control), but no statistical reduction by carvedilol was observed at 24 hours (Fig. 4B). This result further indicates that carvedilol is not merely acting as a sunscreen as both the pre- and post-UVB exposure treatment blocked CPD formation, with the posttreatment displaying slightly less CPD.

The short-term increase in dorsal skin bifold thickness is likely due to an inflammatory reaction to UV. Therefore, the effect of carvedilol on UV-induced IL1β (gene symbol: Il1b, Fig. 4C) and IL6 (gene symbol: Il6, Fig. 4D) expression was examined via quantitative RT-PCR. UV markedly increased IL1β and IL6 levels. Only the postCAR group statistically decreased IL1β and IL6, while pretreatment with carvedilol tended to show lower levels of both IL1β and IL6. Similarly, Western blots for cyclooxygenase 2 (COX-2; Fig. 4E) demonstrate that UV greatly increases COX-2 levels and similarly only postCAR group statistically decreased COX-2 levels (Fig. 4F).

Effects of topically applied carvedilol or 4-OHC on chronic UV-induced skin tumorigenesis in mice

The encouraging result in the short-term model motivated us to further investigate the chemopreventive activity of carvedilol in a murine skin carcinogenesis model. SKH-1 mice were topically treated for 2 weeks with 200 μL vehicle control (acetone), carvedilol (10 μmol/L in acetone), or 4-OHC (10 μmol/L in acetone). The mice were next irradiated by gradually increasing levels of UV radiation from 50 mJ/cm^2 to 150 mJ/cm^2 three times a week for 25 weeks to induce skin tumors as has been documented previously (31). The drug treatment was applied immediately after each UV exposure to minimize sunscreen effects. At week 15,

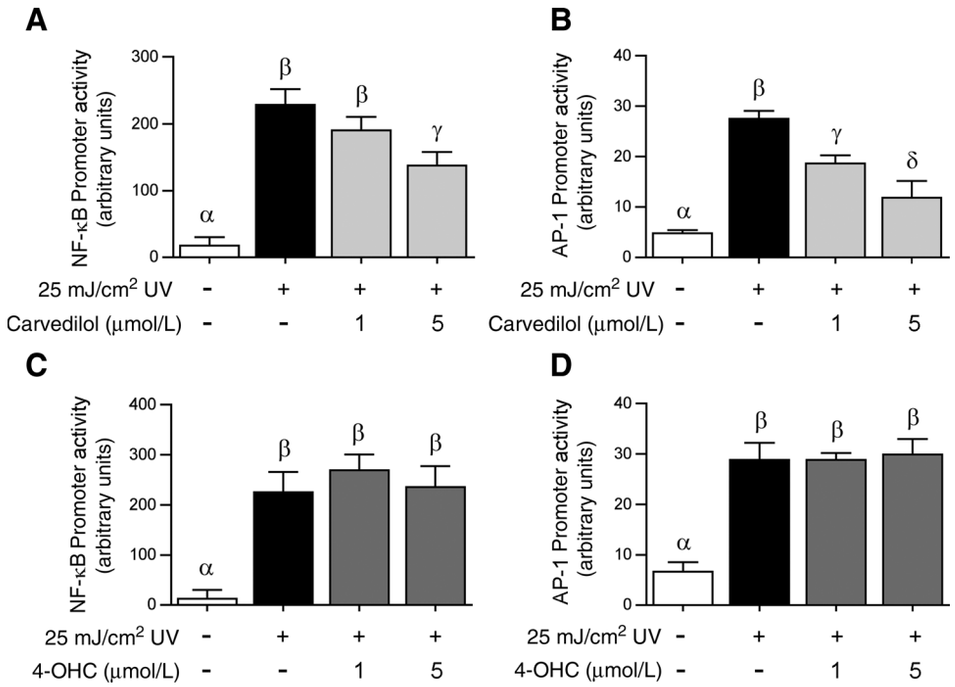

Figure 3.
Effect of carvedilol and 4-OHC on UV-induced NF-κB and AP-1 transcription factors. Effect of carvedilol on UV-induced NF-κB (**A**) and AP-1 (**B**) transactivation, as well as 4-OHC on UV-induced NF-κB (**C**) and AP-1 (**D**) transactivation. HEK-293 cells expressing exogenously transfected AP-1 or NF-κB luciferase reporter and *Renilla* control reporter were treated with vehicle, 25 mJ/cm^2 UV, carvedilol or 4-OHC following UV for 5 or 24 hours for NF-κB and AP-1 assays, respectively. Data are expressed as mean ± SD; $n = 3$. Bars with different Greek letters are statistically different ($P < 0.05$) as per one-way ANOVA with Tukey–Kramer *post hoc* test.

tumors became visible on both acetone (vehicle control) and 4-OHC (sunscreen control) groups, whereas carvedilol-treated animals showed a 3-week delayed onset of tumor incidence. Following this delayed start of tumorigenesis, the median incident week, tumors per mouse, and tumor diameter were statistically lower in the carvedilol group compared with the vehicle control and sunscreen control groups (Table 1). Aside from number and size of tumors, the tumors were visibly worse in the vehicle and sunscreen control groups (Fig. 5A). Additionally, in the vehicle and 4-OHC groups, one animal per group carried severe tumors which required immediate attention by IACUC and was euthanized early due to rapid tumor progression. Because there was no difference between the two controls, pathological identification of tumor type was only conducted on the UV and UV + carvedilol treated groups. Given the marked reductions in tumor formation, it is not surprising that the grade of measurable lesion is more severe in UV-treated mice than those treated with carvedilol after UV exposure (Fig. 5B). At week 25, the acetone group comprised of mice with 6.25 % poorly differentiated squamous cell carcinoma (pSCC) and 50% well differentiated SCC (wSCC) of the total tumors, whereas in the carvedilol group, no pSCC but only 33% wSCC were observed. Lastly, Cox regression analysis indicates that carvedilol slows the appearance of tumors compared with control, $P = 0.0159$; moreover, the rate of tumor appearance on the vehicle and the sunscreen control groups was similar with 4-OHC–treated mice being slightly worse, $P = 0.1746$ (Fig. 5C).

Discussion

The present study is a follow-up investigation of our previous report of the cancer chemopreventive effects of carvedilol (29). The key finding is that carvedilol protects skin against harmful effects induced by UV which is a well-known cause for skin cancer. To the best of our knowledge, this is the first study to demonstrate that a β-blocker, commonly used for cardiovascular diseases, attenuated UV-induced skin tumor development and other molecular changes.

A pitfall with experiments involving UV is that the potential UV absorption properties of test agents may result in a false positive testing result. Therefore, an important and novel method used in this study is the inclusion of a sunscreen control based on the UV absorption properties of the experimental agent (carvedilol). The rationale for the sunscreen control is that if a test agent absorbs UV, it will have a sunscreen effect because the mechanism of action for commercial sunscreens is to absorb UV prior to the tissue absorbing UV. UV absorption is not uncommon for compounds under investigation as skin chemopreventive agents (35). For example, caffeine and its analogues display both sunscreen- and cancer-preventive effects on skin (36). According to the presence of the methoxybenzene ring and carbazole moieties (Fig. 1A), carvedilol was predicted to absorb UV, and the UV spectrum analysis showed that the carbazole moiety appears to be responsible for most of carvedilol-mediated UV absorption because 4-OHC absorbs essentially the same UV spectrum as carvedilol (Fig. 1A). 4-OHC lacks the required β-ethanolamine component of β-blockers, so it is not a β-blocker. However, it is unclear whether the chemopreventive properties of carvedilol are attributed to the β-blocking property. To evaluate 4-OHC's chemopreventive activity, the concentration-response effects of carvedilol and 4-OHC on EGF-mediated transformation of JB6 P$^+$ cells were compared. Obviously, when using EGF as the tumor promoter, the cells are not exposed to UV irradiation; thus, UV absorption is not a factor in this experiment. Because 4-OHC does not inhibit EGF-mediated transformation of JB6 P$^+$ cells (Fig. 1B), 4-OHC was next compared with carvedilol on UV-induced cell transformation. In this

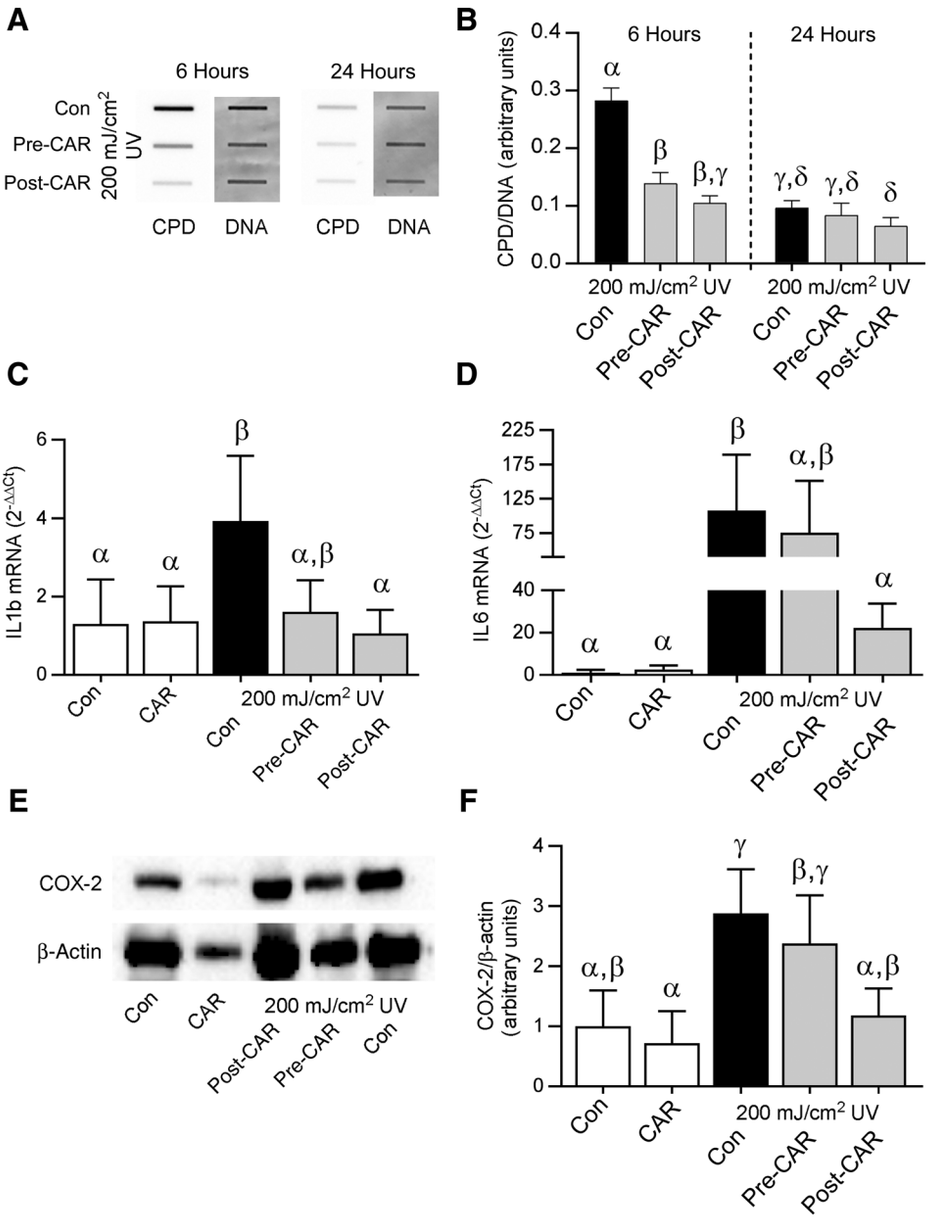

Figure 4.
Effect of carvedilol on short-term high-intensity UV radiation. **A,** Representative slot blot for CPD. Each band represents DNA from one mouse from each treatment group. Genomic DNA was isolated from the dorsal skin of mice irradiated with 200 mJ/cm^2 UV as well as 2 hour pre- or immediately posttreated with 10 μmol/L carvedilol. **B,** CPD data are expressed as mean ± SD; $n = 4$. Bars with different Greek letters are statistically different ($P < 0.05$) as per two-way ANOVA with Tukey–Kramer *post hoc* test. qPCR results from skin samples of the 6-hour group for IL-1β (**C**) and IL-6 (**D**). β-Actin was used as a normalization control, and data are expressed as mean ± SD; $n = 4$ to 8. Bars with different Greek letters are statistically different ($P < 0.05$) as per one-way ANOVA with Kruskal–Wallis multiple-comparison Z-value *post hoc* test. **E,** Representative Western blot for COX-2 and β-actin from skin samples of the 6-hour group. **F,** Radiometric quantification of COX-2 levels in skin samples of the 6-hour group. Data are expressed as mean ± SD; $n = 2$ (Con) and 4 for all others. Bars with different Greek letters are statistically different ($P < 0.05$) as per one-way ANOVA with Tukey–Kramer *post hoc* test.

experiment, carvedilol or 4-OHC was added to the culture media and incubated with cells during the experimental course of 8 weeks. The cells were washed once and incubated in PBS right before each UV exposure; after exposure the cells were reexposed to culture media containing drugs. Although carvedilol or 4-OHC was not present in PBS when the cells were irradiated, the observed protective effects of 4-OHC suggest that the compounds were retained on the cell surface during

Table 1. Effects of topical carvedilol or 4-OHC treatment on the emergence and progression of UV-induced skin tumors

Parameter	Vehicle	Carvedilol	4-OHC	ANOVA *P*
Mice in experiment	10	9[a]	10	
Total number of tumors at the end of experiment[b]	29	13	29	
Tumors per mouse[c]	$3 \pm 1^{\alpha}$	$1 \pm 1^{\beta}$	$3 \pm 1^{\alpha}$	0.004906
Tumor diameter (mm)[d]	$4.26 \pm 2.21^{\alpha}$	$1.96 \pm 1.33^{\beta}$	$3.72 \pm 0.65^{\alpha}$	0.010389
Median incidence week[c]	$20 \pm 3^{\alpha}$	$24 \pm 2^{\beta}$	$18 \pm 2^{\alpha}$	0.009435

[a]One mouse developed an infection of the skin and was excluded from the analysis.
[b]Tumors counted as any mass having a diameter of at least 1 mm before sacrificing the mouse.
[c]Data expressed as median ± MAD; values with different Greek letters are statistically different ($P < 0.05$) as per one-way ANOVA with Kruskal–Wallis Z *post hoc* test.
[d]Data expressed as mean ± SD; values with different Greek letters are statistically different ($P < 0.05$) as per one-way ANOVA with Kruskal–Wallis Z *post hoc* test.

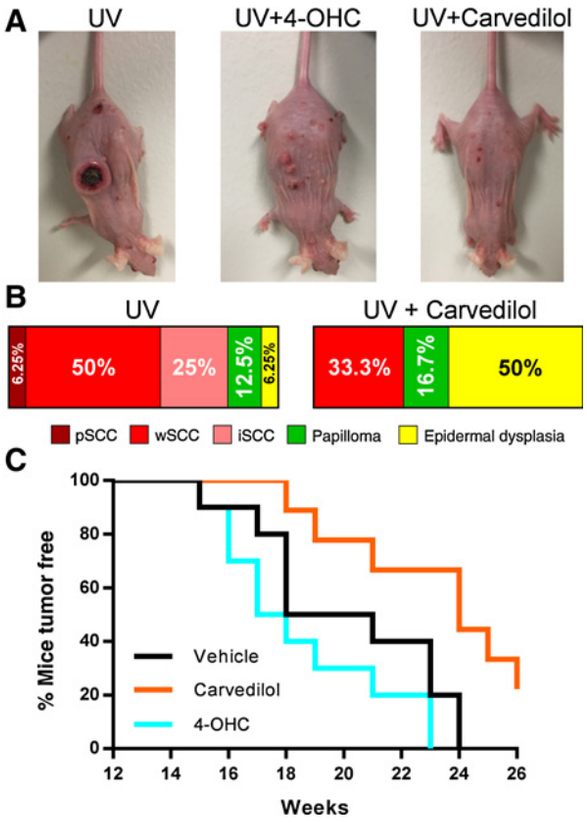

Figure 5.

Effect of carvedilol and 4-OHC on the development of skin tumors in mice. **A,** Representative appearance of mice in each UV-exposure group at week 26. **B,** Summary of the skin lesions in UV- and carvedilol-treated groups. Epidermal lesions were identified as epidermal dysplasia, papilloma, and squamous cell carcinoma (SCC) that was subdivided into three categories: poorly differentiated (pSCC), well differentiated (wSCC), and *in situ* (iSCC). **C,** Cox regression analysis of the percentage of mice not bearing tumors; $P = 0.0159$ for carvedilol versus control and $P = 0.1746$ for 4-OHC versus control.

the washing and contributed to a sunscreen effect. These data demonstrate the need for a sunscreen control. Thus, for the duration of the studies involving UV, sunscreen effects were avoided by treating the cells or animals after UV exposure, and/or by including 4-OHC as control.

In the luciferases assays, when carvedilol and 4-OHC were administered after UV exposure, we obtained the expected results that carvedilol, but not 4-OHC, prevented UV-induced transcriptional activity of NF-κB and AP-1 (Fig. 3). Therefore, treatment after UV is an optimal approach to evaluate carvedilol's chemopreventive effects. Similar approaches can be used for other compounds, as an appropriate sunscreen control may not be easily found for all test agents. Both AP-1 and NF-κB play a causal role in tumor promotion and UV-induced inflammation (37) and are major mediators for development of human skin cancer (38, 39). Therefore, the anticancer mechanism of carvedilol may involve inhibition of AP-1 and NF-κB pathways, although the signaling cascade requires further investigation.

Cellular assays offer simple modes for screening compounds, but do not recapitulate carcinogenesis within a heterogeneous tissue like the skin. Thus, to examine carvedilol's effects on UV-induced DNA damage and skin inflammation, a short protocol similar to what is used in cell culture was applied to SKH-1 mice (Fig. 4). Because the luciferase assay showed that 4-OHC lacked any effect, 4-OHC was not used in the short-term studies. However, two treatment modalities were used: pre- and post-exposure treatments. These two groups mirror a prophylactic treatment, such as the use of sunscreen, and a treatment for a sunburn, respectively. Skin bifold measurements demonstrate that there are rapid changes in skin thickness due to UV exposure in all groups. Carvedilol only statistically reduced skin thickness when treated after UV exposure, and this was detected only after 24 hours. Contrarily, DNA damage, as measured by CPD formation, was statistically reduced within 6 hours by both pre- and posttreatment with carvedilol. Rapid changes in skin thickness are most likely due to the skin hyperplasia and inflammation (40). Posttreatment with carvedilol inhibited UV-induced IL1β and IL6 mRNA production and attenuated COX-2 expression. In each case, pretreatment showed no statistical effect. The difference in pre- and posttreatment at the molecular level is mirrored in the skin thickness assay, suggesting the changes seen at 6 hours contribute to the reduced skin thickness observed at 24 hours. The lack of an effect of pretreatment is not completely understood, but two possibilities underlie the lack of effect at the molecular level. First, the time difference from carvedilol administration to tissue collection between the two modalities is two hours, which is a long time when considering most signaling cascades are measured in minutes. Following UV exposure, the pharmacological actions of carvedilol, such as free radical scavenging, may take place in minutes. Second, UV may enhance the degradation of carvedilol, thus reducing its efficacy. The cellular assays and CPD assay suggest that it can work as a sunscreen, but that may preclude pharmacological actions as the compound could be altered by the UV radiation. Although more studies are necessary to decipher the mechanism of carvedilol in CPD formation, the data clearly indicate that carvedilol is either preventing DNA damage or enhancing repair *in vivo*. CPD assays were attempted in JB6 P^+ cells, but carvedilol failed to prevent CPD formation (data not shown). This suggests that the effect of carvedilol on CPD formation is not a direct effect on the cells, but due to altering the system or microenvironment that indirectly reduces DNA damage or enhances repair. Regardless of the mechanism(s), the short-term experiments indicate that carvedilol would be best used after exposure to UV irradiation—a sunburn treatment.

The short-term UV experiment utilizing 200 mJ/cm^2 UV irradiation is a high dose and does not represent progression of skin cancer that, in humans, can occur after decades of sub-erythema exposure to UV irradiation. Fortunately, mice can model this progression in months, not decades, with repeated low, sub-erythema, doses of UV irradiation. As predicted by the short-term studies, post-exposure treatment with carvedilol protected against UV induced skin carcinogenesis, and 4-OHC, the sunscreen control, had no effect (Table 1 and Fig. 5). The 25-week exposure precludes investigating molecular mechanisms but provides a clinically relevant model to determine if carvedilol is truly a chemopreventive agent. These data confirm that carvedilol is protective when applied after UV exposure. However, further studies are required to find the optimal dose and identify the window after UV exposure that carvedilol remains an effective chemopreventive agent.

β-Blockers, i.e., β-adrenergic receptor antagonists, are usually prescribed for cardiovascular disorders. Recently the role of β-blockers has been reported in preclinical and clinical oncology studies (for reviews, see refs. 1 and 41). However, few studies examined the role of β-blockers in cancer prevention, and fewer examined skin cancer. Foreshadowing the results presented herein are studies demonstarting that chronic stress increased susceptibility to UV-induced SCC in SKH-1 mice through the modulation of immune system and DNA repair (42, 43). Chronic stress leads to activation of the β-ARs (43); thus, β-blockers should help reduce stress-associated SCC. Therefore, carvedilol may help reduce SCC *in vivo* by multiple mechanisms, not only through antitransformation of the epidermis but also by blocking stress-related activation of β-ARs and immunosuppression.

The effects of carvedilol in some of the experiments on cell culture and in mice were not drastic, although many of these changes are statistically significant. Future studies are necessary to explore possibilities to enhance carvedilol's chemopreventive effects. One example includes testing more doses (in this study we mainly examined 1, 5, and 10 μmol/L) and it is feasible to increase the doses for topical treatment. Alternative approach is to use carvedilol analogues to determine if a compound can be identified with greater chemopreventive activity. The third method is to use skin targeting drug delivery system that concentrates carvedilol in the skin layers.

Taken together, although carvedilol acts as a sunscreen, the collective data demonstrate that carvedilol's chemopreventive activity is pharmacological and not merely a sunscreen effect. These results are supported by a large population-based cohort study where long-term carvedilol use showed benefits relating to significant reduction of cancer risk across all cancer types (25). Based on our data and published evidence about the role of β-AR signaling in cancer, carvedilol may be a novel cancer-preventive agent targeting all the three stages of skin carcinogenesis. Topical carvedilol application should be considered as a novel treatment for skin cancer prevention. Also, because carvedilol is an FDA-approved drug for treating chronic cardiovascular diseases with evidence of safety in long-term use, these results may be readily translated into clinical trials as a new approach for skin cancer chemoprevention. One obstacle for the use of carvedilol for preventive purpose is its potential cardiovasuclar effects. Further studies should determine whether the β-blocking moiety of carvedilol is responsible for the chemopreventive effects and whether β-ARs are the target for such effects. Additionally, delivery systems can be developed to trap carvedilol in the skin localizing the pharmacological action and preventing cardiovascular effects.

Disclosure of Potential Conflicts of Interest

No potential conflicts of interest were disclosed.

Authors' Contributions

Conception and design: K.M. Huang, E. Oiyemhonlan, F.L. Meyskens Jr., B.T. Andresen, Y. Huang

Development of methodology: K.M. Huang, S. Liang, Y. Huang

Acquisition of data (provided animals, acquired and managed patients, provided facilities, etc.): K.M. Huang, S. Yeung, K.H. Cleveland, C. Parsa, R. Orlando, B.T. Andresen, Y. Huang

Analysis and interpretation of data (e.g., statistical analysis, biostatistics, computational analysis): K.M. Huang, S. Liang, E. Oiyemhonlan, R. Orlando, F.L. Meyskens Jr., B.T. Andresen, Y. Huang

Writing, review, and/or revision of the manuscript: S. Liang, E. Oiyemhonlan, C. Parsa, R. Orlando, F.L. Meyskens Jr., B.T. Andresen, Y. Huang

Administrative, technical, or material support (i.e., reporting or organizing data, constructing databases): S. Liang, S. Yeung, E. Oiyemhonlan, B.T. Andresen

Study supervision: B.T. Andresen, Y. Huang

Other (preparation and processing and interpretative study of tissues): R. Orlando

Acknowledgments

We would like to thank Dr. David Sanchez (Western University of Health Sciences, Pomona, California) for the gift of pGL4.22-AP1. Additionally, we would like to thank Dr. Norman A. Andresen for aiding in designing and constructing the UV exposure chamber.

Grant Support

E. Oiyemhonlan was supported by Western University of Health Sciences Summer Student Fellowship Grant.

Received May 2, 2017; revised July 20, 2017; accepted August 8, 2017; published OnlineFirst August 15, 2017.

References

1. Eng JW, Kokolus KM, Reed CB, Hylander BL, Ma WW, Repasky EA. A nervous tumor microenvironment: the impact of adrenergic stress on cancer cells, immunosuppression, and immunotherapeutic response. Cancer Immunol Immunother 2014;63:1115–28.
2. Hara MR, Kovacs JJ, Whalen EJ, Rajagopal S, Strachan RT, Grant W, et al. A stress response pathway regulates DNA damage through beta2-adrenoreceptors and beta-arrestin-1. Nature 2011;477:349–53.
3. Flint MS, Baum A, Chambers WH, Jenkins FJ. Induction of DNA damage, alteration of DNA repair and transcriptional activation by stress hormones. Psychoneuroendocrinology 2007;32:470–9.
4. Flint MS, Baum A, Episcopo B, Knickelbein KZ, Liegey Dougall AJ, Chambers WH, et al. Chronic exposure to stress hormones promotes transformation and tumorigenicity of 3T3 mouse fibroblasts. Stress 2013;16:114–21.
5. Seiffert K, Hosoi J, Torii H, Ozawa H, Ding W, Campton K, et al. Catecholamines inhibit the antigen-presenting capability of epidermal Langerhans cells. J Immunol 2002;168:6128–35.
6. Gillbro JM, Marles LK, Hibberts NA, Schallreuter KU. Autocrine catecholamine biosynthesis and the beta-adrenoceptor signal promote pigmentation in human epidermal melanocytes. J Invest Dermatol 2004;123:346–53.
7. Scarparo AC, Visconti MA, de Oliveira AR, Castrucci AM. Adrenoceptors in normal and malignant human melanocytes. Arch Dermatol Res 2000;292:265–7.
8. Moretti S, Massi D, Farini V, Baroni G, Parri M, Innocenti S, et al. beta-adrenoceptors are upregulated in human melanoma and their activation releases pro-tumorigenic cytokines and metalloproteases in melanoma cell lines. Lab Invest 2013;93:279–90.
9. Sivamani RK, Porter SM, Isseroff RR. An epinephrine-dependent mechanism for the control of UV-induced pigmentation. J Invest Dermatol 2009;129:784–7.
10. Powe DG, Voss MJ, Zanker KS, Habashy HO, Green AR, Ellis IO, et al. Beta-blocker drug therapy reduces secondary cancer formation in breast cancer and improves cancer specific survival. Oncotarget 2010;1:628–38.
11. Luthy IA, Bruzzone A, Pinero CP, Castillo LF, Chiesa IJ, Vazquez SM, et al. Adrenoceptors: non-conventional target for breast cancer? Curr Med Chem 2009;16:1850–62.
12. Barron TI, Sharp L, Visvanathan K. Beta-adrenergic blocking drugs in breast cancer: a perspective review. Ther Adv Med Oncol 2012;4:113–25.

13. Barron TI, Connolly RM, Sharp L, Bennett K, Visvanathan K. Beta blockers and breast cancer mortality: a population- based study. J Clin Oncol 2011; 29:2635–44.
14. Melhem-Bertrandt A, Chavez-Macgregor M, Lei X, Brown EN, Lee RT, Meric-Bernstam F, et al. Beta-blocker use is associated with improved relapse-free survival in patients with triple-negative breast cancer. J Clin Oncol 2011;29:2645–52.
15. Grytli HH, Fagerland MW, Fossa SD, Tasken KA, Haheim LL. Use of beta-blockers is associated with prostate cancer-specific survival in prostate cancer patients on androgen deprivation therapy. Prostate 2013;73:250–60.
16. Grytli HH, Fagerland MW, Fossa SD, Tasken KA. Association between use of beta-blockers and prostate cancer-specific survival: a cohort study of 3561 prostate cancer patients with high-risk or metastatic disease. Eur Urol 2014;65:635–41.
17. Diaz ES, Karlan BY, Li AJ. Impact of beta blockers on epithelial ovarian cancer survival. Gynecol Oncol 2012;127:375–8.
18. Jansen L, Hoffmeister M, Arndt V, Chang-Claude J, Brenner H. Stage-specific associations between beta blocker use and prognosis after colorectal cancer. Cancer 2014;120:1178–86.
19. Wang HM, Liao ZX, Komaki R, Welsh JW, O'Reilly MS, Chang JY, et al. Improved survival outcomes with the incidental use of beta-blockers among patients with non-small-cell lung cancer treated with definitive radiation therapy. Ann Oncol 2013;24:1312–9.
20. Lemeshow S, Sorensen HT, Phillips G, Yang EV, Antonsen S, Riis AH, et al. beta-Blockers and survival among Danish patients with malignant melanoma: a population-based cohort study. Cancer Epidemiol Biomarkers Prev 2011;20:2273–9.
21. De Giorgi V Grazzini M, Gandini S, Benemei S, Lotti T, Marchionni N, et al. Treatment with beta-blockers and reduced disease progression in patients with thick melanoma. Arch Intern Med 2011;171:779–81.
22. Bangalore S, Kumar S, Kjeldsen SE, Makani H, Grossman E, Wetterslev J, et al. Antihypertensive drugs and risk of cancer: network meta-analyses and trial sequential analyses of 324,168 participants from randomised trials. Lancet Oncol 2011;12:65–82.
23. Algazi M, Plu-Bureau G, Flahault A, Dondon MG, Le MG. [Could treatments with beta-blockers be associated with a reduction in cancer risk?]. Rev Epidemiol Sante Publique 2004;52:53–65.
24. Grossman E, Messerli FH, Goldbourt U. Antihypertensive therapy and the risk of malignancies. Eur Heart J 2001;22:1343–52.
25. Lin CS, Lin WS, Lin CL, Kao CH. Carvedilol use is associated with reduced cancer risk: a nationwide population-based cohort study. Int J Cardiol 2015;184:9–13.
26. Yue TL, Cheng HY, Lysko PG, McKenna PJ, Feuerstein R, Gu JL, et al. Carvedilol, a new vasodilator and beta adrenoceptor antagonist, is an antioxidant and free radical scavenger. J Pharmacol Exp Ther 1992;263:92–8.
27. Yue TL, McKenna PJ, Ruffolo RR Jr., Feuerstein G. Carvedilol, a new beta-adrenoceptor antagonist and vasodilator antihypertensive drug, inhibits superoxide release from human neutrophils. Eur J Pharmacol 1992; 214:277–80.
28. Calo LA, Semplicini A, Davis PA. Antioxidant and antiinflammatory effect of carvedilol in mononuclear cells of hypertensive patients. Am J Med 2005;118:201–2.
29. Chang A, Yeung S, Thakkar A, Huang KM, Liu MM, Kanassatega RS, et al. Prevention of skin carcinogenesis by the beta-blocker carvedilol. Cancer Prev Res (Phila) 2015;8:27–36.
30. Yang S, Misner B, Chiu R, Meyskens FL Jr.Common and distinct mechanisms of different redox-active carcinogens involved in the transformation of mouse JB6P+ cells. Mol Carcinog 2008;47:485–91.
31. Dickinson SE, Melton TF, Olson ER, Zhang J, Saboda K, Bowden GT. Inhibition of activator protein-1 by sulforaphane involves interaction with cysteine in the cFos DNA-binding domain: implications for chemoprevention of UVB-induced skin cancer. Cancer Res 2009; 69:7103–10.
32. Afaq F, Adhami VM, Ahmad N, Mukhtar H. Inhibition of ultraviolet B-mediated activation of nuclear factor kappaB in normal human epidermal keratinocytes by green tea Constituent (-)-epigallocatechin-3-gallate. Oncogene 2003;22:1035–44.
33. Hart RW, Setlow RB, Woodhead AD. Evidence that pyrimidine dimers in DNA can give rise to tumors. Proc Natl Acad Sci U S A 1977;74: 5574–8.
34. Wilgus TA, Koki AT, Zweifel BS, Kusewitt DF, Rubal PA, Oberyszyn TM. Inhibition of cutaneous ultraviolet light B-mediated inflammation and tumor formation with topical celecoxib treatment. Mol Carcinog 2003; 38:49–58.
35. Lu YP, Lou YR, Xie JG, Peng QY, Zhou S, Lin Y, et al. Caffeine and caffeine sodium benzoate have a sunscreen effect, enhance UVB-induced apoptosis, and inhibit UVB-induced skin carcinogenesis in SKH-1 mice. Carcinogenesis 2007;28:199–206.
36. Conney AH, Lu YP, Lou YR, Kawasumi M, Nghiem P. Mechanisms of caffeine-induced inhibition of UVB carcinogenesis. Front Oncol 2013; 3:144.
37. Dhar A, Young MR, Colburn NH. The role of AP-1, NF-kappaB and ROS/NOS in skin carcinogenesis: the JB6 model is predictive. Mol Cell Biochem 2002;234–235:185–93.
38. Huang C, Ma WY, Hanenberger D, Cleary MP, Bowden GT, Dong Z. Inhibition of ultraviolet B-induced activator protein-1 (AP-1) activity by aspirin in AP-1-luciferase transgenic mice. J Biol Chem 1997;272: 26325–31.
39. Tobin D, van Hogerlinden M, Toftgard R. UVB-induced association of tumor necrosis factor (TNF) receptor 1/TNF receptor-associated factor-2 mediates activation of Rel proteins. Proc Natl Acad Sci U S A 1998;95: 565–9.
40. Clydesdale GJ, Dandie GW, Muller HK. Ultraviolet light induced injury: immunological and inflammatory effects. Immunol Cell Biol 2001; 79:547–68.
41. Chung JF, Lee SJ, Sood AK. Immunological and pleiotropic effects of individual beta-blockers and their relevance in cancer therapies. Expert Opin Investig Drugs 2016;25:501–5.
42. Saul AN, Oberyszyn TM, Daugherty C, Kusewitt D, Jones S, Jewell S, et al. Chronic stress and susceptibility to skin cancer. J Natl Cancer Inst 2005;97:1760–7.
43. Yang EV, Eubank TD. The impact of adrenergic signaling in skin cancer progression: possible repurposing of beta-blockers for treatment of skin cancer. Cancer Biomark 2013;13:155–60.